

Robotic Deburring of parts with Unknown Geometry

H. Kazerooni
M. G. Her

Mechanical Engineering Department
University of Minnesota
Minneapolis, MN 55455

Abstract

The work presented here is an approach in robotic deburring of two dimensional parts with unknown geometry. Two problems have been addressed in this paper: tracking the the part contour, and control of the metal removal process. The tracking mechanism is a roller bearing mounted on a force sensor at the robot endpoint. The tracking control employs the force measured by this force sensor to find the normal to the part surface, while the deburring algorithm uses another set of contact forces (cutting forces generated by the cutter) to develop a stable metal removal. A set of experimental results is given to verify the effectiveness of the approach.

1. Introduction

Two problems are involved in development of an automated robotic deburring of parts with unknown geometry: 1) the design of an appropriate procedure for a stable metal removal, and 2) the development of a stable control method for tracking the edge of the parts with unknown geometry. Although these two problems for a particular application may be merged together, we separate them in the sense of hardware and control method. This separation allows us to arrive at improved results for both tracking and metal removal. References 3,4, 7 and 12, list various effective robotic deburring methods where the knowledge of the part geometry is essential. Section 2 describes a tracking control method, while section 3 is devoted to development of the deburring method.

2. Tracking of The Parts with Unknown Geometry

We define tracking a two dimensional part by a robot as a stable maneuver in which the robot endpoint always remains in contact with the part. Note that the above definition is independent of the type of the geometric knowledge of the part. In fact, the geometric knowledge of the part may not be exactly available prior to the tracking maneuver. The above definition is also independent of the control strategy and it implicitly states the stability of the system and consequently the boundedness of the contact forces. Figure 1 shows the schematic of tracking an edge of a part. Although the regulation of the contact force in the direction normal to the part surface is an attractive choice in many industrial applications, one is not restrained to do so in tracking a two dimensional surface¹. There are two components in performing the tracking of a part with unknown geometry: the collection of the part geometry and the control method. In section 2.1 we describe one method of collecting the environment geometry while section 2.2 is devoted to the robot control method and its stability.

2.1 A Method for Collecting the Part Geometry

In this section, we describe a practical method of collecting the part geometry based on the measurement of the interaction forces between the part and the robot. A two

¹One may develop impedance control in the direction normal to the part such that the robot is compliant and therefore the normal force remains bounded.

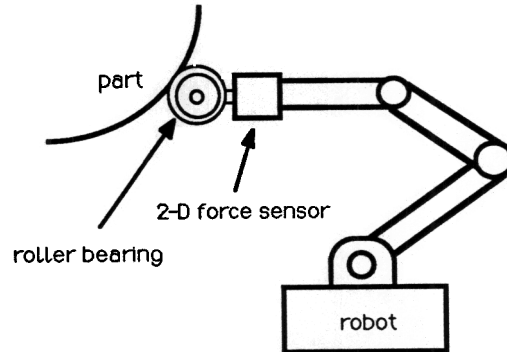


Figure 1: A roller bearing mounted on a force sensor can be used as an end-effector in tracking a part.

dimensional force sensor mounted on a roller bearing can provide sufficiently accurate force information for tracking purposes. Figure 2 shows the detailed schematic of the force sensor assembly mounted on a robot. We assume that the part is mounted on a stationary platform. The tracking force imposed on the part by the robot, t , consists of two components; the compression force, t_n , in the direction normal to the part surface, and the friction force, t_t , tangent to the part (Figure 3). If the friction between the roller and part surface is of the Coulomb type then:

$$t_t = \mu t_n \quad (1)$$

where μ is the coefficient of dry friction. If the measured forces in the global coordinate frame are t_x and t_y then equality 2 can be achieved by inspection of Figure 3.

$$\begin{pmatrix} t_x \\ t_y \end{pmatrix} = R \begin{pmatrix} t_n \\ t_t \end{pmatrix} \quad (2)$$

$$\text{where: } R = \begin{pmatrix} -\sin(\alpha) & \cos(\alpha) \\ \cos(\alpha) & \sin(\alpha) \end{pmatrix}$$

α is the angle between the normal to the part and the y axis in the global coordinate frame. Equations 1 and 2 taken together result in equation 3 for the value of α .

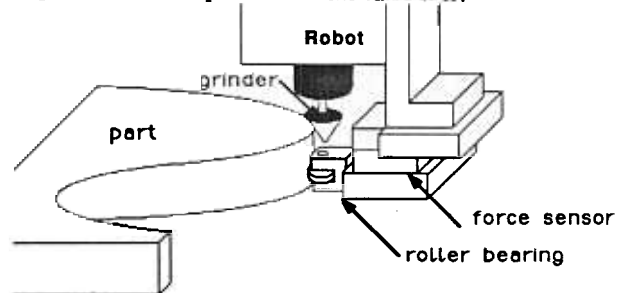


Figure 2: The Schematic of the Force Sensor Assembly

$$\tan(\alpha) = \frac{(\mu t_y - t_x)}{(\mu t_x + t_y)} \quad (3)$$

$$\text{or: } \alpha = \tan^{-1} \frac{(\mu t_y - t_x)}{(\mu t_x + t_y)} \quad (4)$$

By measuring t_x and t_y , one can calculate α if μ is known². Exact calculation of α requires a precise value of μ . Since the friction between the roller bearing and the part surface is very small, then one can arrive at an approximate value for α from equation 5. (We will experimentally verify the small size of μ in Section 2.2, Figure 6).

$$\alpha \approx \tan^{-1} \frac{t_x}{t_y} \quad (5)$$

In practice, μ is not a zero quantity and any small perturbation of μ will cause α to deviate from its value given by equation 5. The sensitivity of α in the presence of the perturbation of μ can be approximated by:

by equation 5. The sensitivity of α in the presence of the perturbation of μ can be approximated by:

$$\delta\alpha = \frac{1}{1+\mu^2} \delta\mu \quad (6)$$

where δ represents a small deviation. $\delta\mu$, for a roller bearing, is a small number which results in a small deviation in α . $\delta\mu=0.01$ results in $\delta\alpha=0.57^\circ$ where $\mu=0$. This sensitivity analysis shows that a simple force sensor assembly allows for a relatively accurate part geometric information.

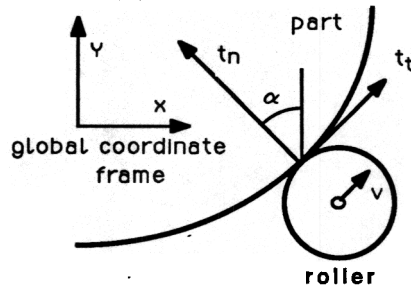


Figure 3: t_t and t_n are tangential and normal forces exerted on the part.

2.2 Control Method for Tracking

In this section, we develop a control method that allows the robot to track the edge of two dimensional parts. Employing the above method for calculation of the surface normal, the control method keeps the normal contact force at a constant quantity. The designer is allowed, however, to assign a velocity command in the tangential direction. We will clarify later in Section 3 that the deburring approach described here assigns a value for tangential velocity.

We assume the robot already has a velocity controller. The fact that most industrial manipulators already have some kind of velocity controller is the motivation behind our approach. Also, a number of methodologies exist for the development of robust velocity controllers for direct and non-direct robot manipulators. In general, the end-point velocity of a robot manipulator that has a velocity controller is a dynamic function of its input trajectory vector, e , and the external force, t . Let G and S be two functions that show the robot endpoint velocity in a global coordinate frame, v , is a function of the input trajectory, e , and the external force, t .

² Note that an equality similar to equation 3 can be derived using the measured forces in the hand coordinate frame rather than the global coordinate frame. For the benefit of consistency throughout the paper we chose to express the measured forces in the global coordinate frame.

$$v = G(e) + S(t)$$

The motion of the robot end-point in response to imposed forces, t , is caused by either structural compliance in the robot³ or by the compliance of the velocity controller. Robot manipulators with velocity controllers are not infinitely stiff in response to external forces (also called disturbances). Even though the velocity controllers of robots are usually designed to follow the trajectory commands and reject disturbances, the robot end-point will move somewhat in response to imposed forces on it. S is called the sensitivity function and it maps the external forces to the robot velocity. For a robot with a "good" velocity controller, S is a mapping with small gain. Non-direct drive robots with high gear ratio also have small sensitivity to external forces. No assumption on the internal structures of $G(e)$ and $S(t)$ is made.

Figure 4 shows one possible example of internal structure of the model represented by equation 7. The robot open loop dynamic equation is $M(\theta)\dot{\theta} + C(\theta, \dot{\theta}) + G_r(\theta) - \tau + J_o^T t$ where $M(\theta)$, $C(\theta, \dot{\theta})$, $G_r(\theta)$ and J_o are the inertia matrix, coriolis, gravity forces and the Jacobian. τ and t are the driving torque and the external forces on the robot. With the help of two mappings, T_1 and T_2 , we define θ_d and $\dot{\theta}$ as the desired velocity and the actual velocity of the robot in the joint coordinate frame. P1 and P2 are computer programs that calculate the best estimated values of nonlinear terms in robot dynamics. K_v is appropriate velocity gain to stabilize the system(13). The system in Figure 4 with two inputs (e and t), and one output, v , can be represented by equation 7. In the analysis of the tracking controller, we employ equation 7 as the basic dynamic equation of the robot that already has a velocity controller. The type of the velocity controller is not of importance at this stage. Regardless of the kind of controller, one can always consider the closed loop system dynamics in terms of the structure of equation 7.

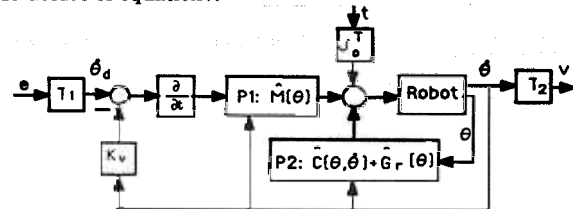


Figure 4: One possible example in development of the velocity controller for a robot with rigid body dynamics. $\hat{M}(\theta)$, $\hat{C}(\theta, \dot{\theta})$ and $\hat{G}_r(\theta)$ are the estimated values (13).

Equation 7 represents an input/output functional relationship. It allows us to incorporate the dynamic behavior of all the elements of the robot. Many industrial robot manipulators already have some kind of velocity controllers. Within the bandwidth of the velocity control, $(0, \omega_0)$, the dynamic behavior of the robot is uncoupled. In other words, for all frequencies in $(0, \omega_0)$, a command in a particular direction will generate a velocity in the commanded direction only. Outside of the robot closed loop bandwidth, the robot dynamics are coupled and a velocity command in a particular direction, in general, may develop velocity deviation in some or all directions. Regarding the above practical issue, we assume G and S are uncoupled functions; G_n and S_n represent the robot dynamic behavior in the direction normal to the part, while G_t and S_t show the dynamics of the robot in the direction tangent to the part. Figure 5 shows the dynamics of the robot and part in

³ In a simple example, if a Remote Center Compliance (RCC) with a linear dynamic behavior is installed at the endpoint of the robot, then S is equal to the reciprocal of stiffness (impedance in the dynamic sense) of the RCC.

the direction normal to the part. E_n represents the dynamic behavior of the part and force sensor in the direction normal to the part. In the simplest case, one can think of E_n as the stiffness of a spring that could possibly model the part stiffness.

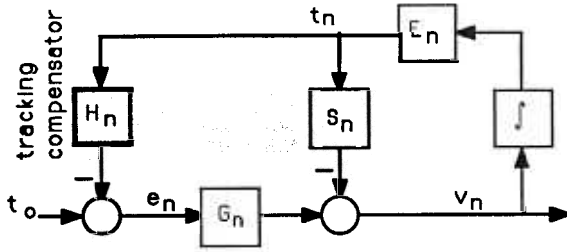


Figure 5: The Block Diagram of the System in Normal Direction When the Robot is in Contact with the Part.

The compensator, H_n , is considered to operate on the contact force, t_n . t_0 is the reference signal representing the desired normal contact force. The compensator output signal subtracted from t_0 is used as the normal input command signal, e_n , for the robot velocity controller.

There are two feedback loops in the system; the inner loop (which is the natural feedback loop), shows how the contact force affects the robot in a natural way when the robot is in contact with the part. The outer feedback loop is the controlled feedback loop. When the robot and the part are in contact, then the value of the contact force and the endpoint velocity of robot are given by t_n and v_n where the following equations are true:

$$v_n = G_n(e_n) - S_n(t_n) \quad (8)$$

$$t_n = E_n(\int v_n) \quad (9)$$

$$e_n = t_0 - H_n t_n \quad (10)$$

If the operators in equations 8,9, and 10 are linear, the transfer function in equation 11 can be obtained to represent the force.

$$t_n = E_n(s + S_n E_n + G_n H_n E_n)^{-1} G_n t_0 \quad (11)$$

E_n , impedance of the part in the normal direction, is a large quantity in comparison with the other parameters in the system. If E_n approaches infinity, then equations 12 and 13 represent the value of t_n and v_n .

$$t_n = (S_n + G_n H_n)^{-1} G_n t_0 \quad (12)$$

$$v_n = 0 \quad (13)$$

Note that S_n and $G_n H_n$ add in equation 12 to develop the total compliancy in the system. $G_n H_n$ represents the electronic compliancy in the robot while S_n models the natural hardware compliancy (such as RCC or the robot structural compliancy) in the system⁴. A large value for H_n develops a compliant robot while a small H_n generates a stiff robot. Reference 9 describes a micro manipulator in which the compliancy in the system is shaped for metal removal application. Equation 12 also shows that a robot with good

⁴ Equation 11 can be rewritten as $t_n = (sE_n^{-1} + S_n + G_n H_n)^{-1} G_n t_0$. Note that the part admittance (1/impedance in the linear domain), E_n^{-1} , the robot sensitivity (1/stiffness in the linear domain), S_n , and the electronic compliancy, $G_n H_n$, add together to form the total sensitivity of the system. If $H_n=0$, then only the admittance of the environment and the robot add together to form the compliancy for the system. By closing the loop via H_n , one can add to the total sensitivity of the system.

tracking capability (small gain for S_n) may generate a large contact force in a particular contact. One cannot choose arbitrarily large values for H_n ; the stability of the closed-loop system of Figure 5 must be guaranteed. To guarantee the stability of the closed-loop system in the nonlinear case, H_n must be chosen such that (reference 11):

$$\|H_n\|_P < \frac{\|e_n\|_P}{\|W_n(e_n)\|_P} \quad (14)$$

Inequality 14 states that the L_P -norm of H_n must be less than the reciprocal of the "magnitude" of the mapping in the forward loop in Figure 5 where $\|\cdot\|_P$ represents the P-norm of a function. $W_n(e_n)$ is the mapping from e_n to t_n . In the linear case, $W_n = E_n(S_n E_n + s)^{-1} G_n$ where all the operators in the system are linear transfer functions. The stability criteria for linear system is:

$$|H_n| < |s G_n^{-1} (S_n/s + 1/E_n)| \quad (15)$$

where $|\cdot|$ denotes the magnitude of the transfer function. The smaller the sensitivity of the robot manipulator is, the smaller H_n must be chosen. Also from inequality 15, the more rigid the part is, the smaller H_n must be chosen. In the "ideal case", no H_n can be found to allow an infinitely rigid robot ($S_n=0$) to interact with an infinitely rigid part ($E_n=\infty$). In other words, for stability of the system shown there must be some compliancy either in robot or in the part. RCC, structural dynamics and the tracking controller stiffness form the compliancy on the robot. An XY table was employed as a simple two dimensional robot to experimentally verify the effectiveness of the tracking method. The XY table holds the part to be tracked while a stationary platform holds the force sensor and the roller bearing. The XY table is powered by two DC motors via a two screw mechanism. The screws are double-helix and 0.2 inch per revolution. Each axis of the table has a simple PID velocity controller. H_n was chosen small enough to guarantee inequality 15. Figure 6 shows the experimental values for normal and tangential forces, t_t and t_n for period of two seconds.

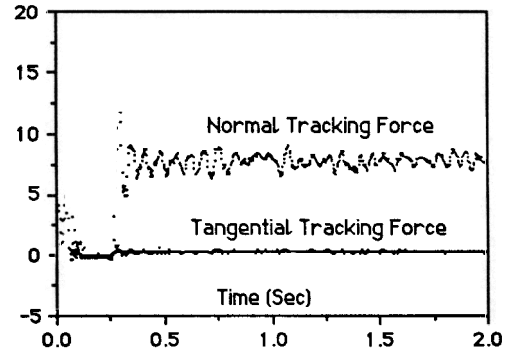


Figure 6: Normal and Tangential Contact Forces in Tracking. The Commanded Velocity in Tangential Direction is 0.5 cm/sec.

3. Deburring Strategy

This section focuses on the deburring mechanics and its required control approach. We start with analysis of the deburring process model in Section 3.1, while Section 3.2 is devoted to the required control strategy for metal removal. The deburring control strategy is independent of the tracking control.

3.1 Process Dynamic Model

This section describes several quantitative and geometric properties of burrs formed in the cutting process. These properties, which are independent of the control algorithm, lead us to development of a simple dynamic model for the cutting process. The control algorithm used in Section 3.2 is benefited by this dynamic model.

The material removal rate (MRR) of a deburring pass is a function of the velocity of the tool bit along the edge and the cross sectional areas of both the chamfer and the burr(7, 10). This relationship can be expressed as:

$$MRR = (A_{\text{chamfer}} + A_{\text{burr}}) V_{\text{tool}} \quad (16)$$

In the deburring process, the cutting force in the tangential direction is proportional to MRR (7,10). For a given constant feedrate, V_{tool} , the tangential force varies very significantly with variation of the burr size; thus whenever the rotary file encounters a large burr, the tangential force increases dramatically. For a given constant feedrate, the normal force stays relatively constant regardless of burr size variation. Figure 7 shows the proportionality of the tangential cutting force, d_t , with MRR when an edge with 45° chamfer is cut.

$$d_t = K \times MRR \quad (17)$$

K depends on the material properties while MRR is a geometric quantity.

For a given depth of cut (0.055") on an edge without a burr, the feedrate was varied and the MRR was measured. As shown in Figure 7, the cutting process requires some minimum tangential force to penetrate the material. The operating point for the experiments is along the linear section of the plot in Figure 7. Since A_{chamfer} is constant in this experiment, the tangential force is therefore proportional to the feedrate. The faster the speed of the tool along the edge is, the larger the tangential contact force will be. The slope of the line in Figure 7 (1016 nt/grams/sec) represents the proportionality of the tangential force with the MRR. Considering the specific mass of steel as 7 grams/cm³, the slope of the line equal to 7112 nt/cm³/sec and represents the proportionality of the contact force with the volumetric MRR. Taking into account the projected tangential area of 0.0098cm², the proportionality of the tangential cutting force with the velocity along the edge is 69.8nt/cm/sec. It requires 69.8nt of tangential force to cut along the edge with the speed of 1cm/sec. Note that the relationship between the cutting force and the speed along the edge represents the dynamic behavior of the process. If the speed of the tool along the edge of the part is kept constant, we expect an increase in the tangential force when the cutting tool encounters a burr along the edge of the part.

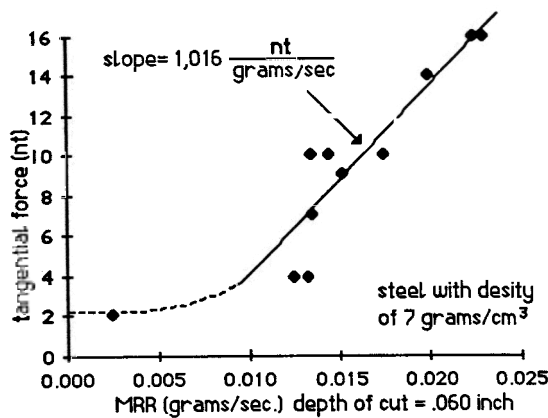


Figure 7: The tangential force is proportional to the material removal rate

3.2 Control Strategy For Deburring

This section is devoted to the control of a robot for deburring tasks only. Suppose the cutting tool is being moved with constant speed by an industrial robot along the edge of a part, then the cutting force will vary significantly because of the variation of the burr size. This cutting force can be resolved into two orthogonal directions as in Figure 8. If the contact force is large due to the size of the burr, a separation of the robot from the part will occur. We desire to develop a self tuning strategy such that the cutting force in the cutting process becomes small when the cutter encounters a burr. A small cutting force guarantees that the cutter stays very close to the part without separation. Consider the deburring of a surface by a robot manipulator; the objective is to use an end-effector to smooth the surface down to the commanded trajectory depicted by the dashed line in Figure 8. It is intuitive to design a position control mechanism for the manipulator with a small sensitivity in the normal direction and a force control in the tangential direction.

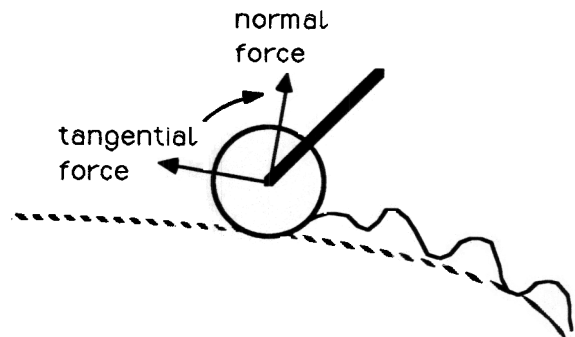


Figure 8: Deburring an Edge; Up Cutting

A trajectory control with small sensitivity in the normal direction causes the end-point of the grinder to reject the cutting forces and stay very close to the commanded trajectory (dashed-line). We define the sensitivity as the ratio of the robot motion to the normal cutting force. Given the volume of the metal to be removed, the desired tolerance in the normal direction prescribes an approximate value for the sensitivity of the trajectory control in the normal direction. In practice, one can develop large loop gains (by employment of several integrators) to gain small sensitivity in the system. One natural way of developing small sensitivity in the system is the employment of the robot in such a configuration that the robot has the highest effective inertia in the normal direction. The high inertia in the normal direction causes the robot to stay very "rigid" in response to interaction forces (1).

As described previously, the force necessary to cut in the tangential direction at a constant traverse speed is approximately proportional to the volume of the metal to be removed. Therefore, the larger the burrs on the surface, the slower the manipulator must move in the tangential direction to maintain a relatively constant tangential force. This is necessary because the slower speed of the end-point along the surface implies a smaller volume of metal to be removed per unit of time, and consequently, less force in the tangential direction. To remove the metal from the surface, the grinder should slow down in response to contact forces with large burrs. The above explanation demonstrates that it is necessary for the end-effector to accommodate the interaction forces along the tangential direction, which directly implies a force control system in the tangential direction. If a designer does not accommodate the interaction forces by developing a force control system in the tangential direction, the large burrs on the surface will produce large contact forces in the tangential direction (equation 17).

It is desired to develop a force control system in the tangential direction so that by varying the velocity of the tool along the edge of the part, a relatively constant cutting force is maintained in the tangential direction. Two problems are associated with large cutting forces in the tangential directions: 1) the cutting tool may stall (if it does not break), and 2) a slight deflection may develop in the end-point position in the normal direction, which might exceed the desired tolerance. This is due to slight coupling of the force between the normal and tangential directions.

The frequency spectrum of the roughness of the surface and the desired translational speed of the robot along the surface determine the frequency range of operation, ω_b . ω_b is the frequency range of the burr seen from the end-effector. The faster the robot end point travels along the edge of the part, the wider ω_b will be. The bandwidth of the control system in the tangential direction must be larger than ω_b . In other words one must travel with an average speed along the edge of the part such that ω_b falls below the bandwidth of the control system. It is clear that the smaller the value for the commanded tangential force is, the slower the robot will move along the edge of the part. In fact if the commanded force in the tangential direction is very small, the tool will not travel along the edge. This is true, because the controller will drive the system with a small speed to reach to a small force. If a large value is commanded for the force in the tangential direction, then the tool will travel with a large contact force in the tangential direction.

Figure 9 illustrates the architecture of the closed-loop control system for the robot in the tangential direction. The detailed description of each operator in Figure 9 is similar to the one shown in Figure 4.

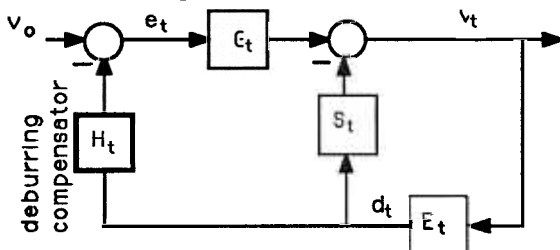


Figure 9: The Closed-Loop Control in Tangential Direction for Deburring

G_t is the transfer function (or a mapping in the nonlinear case) that represents the dynamic behavior of the robot with a velocity controller in the tangential direction. The input to G_t is the input velocity, v_0 . v_t is the robot velocity in the tangential direction. G_t can be calculated experimentally or analytically. Note that G_t is approximately equal to the unity for the frequencies within its bandwidth. In other words, we assume that a velocity controller has been designed for the robot such that it closely follows all the trajectories with frequency components within the bandwidth of G_t . ω_0 represents the bandwidth of G_t .

S_t , the sensitivity transfer function (or a mapping in the nonlinear case), represents the relationship between the external force on the end point and the end point velocity. This velocity deviation is due to either structural compliance in the end-effector mechanism or the velocity controller compliance. To obtain good velocity control, S_t must be quite "small". The notion of "small" can be regarded in the singular value sense when S_t is a transfer function matrix. L_p -norm (6) can be considered to show the size of S_t in the nonlinear case. S_t shows how good a velocity control is.

E_t represents the dynamic behavior of the part. In the

linear case, E_t has been measured from the slope of the plot in Figure 8 and its value is equal to 69.8 nt/cm/sec. In general, one can consider a nonlinear function to characterize E_t .

H_t is the compensator to be designed. The input to this compensator is the tangential deburring force. The compensator output signal is subtracted from the input tangential velocity, v_t , to give the error signal, e_t , as the input velocity for the robot manipulator in the tangential direction. The value of the tangential force and the end-point tangential velocity of the robot are given by equations 18 and 19.

$$d_t = E_t [1 + S_t E_t + G_t H_t E_t]^{-1} G_t v_0 \quad (18)$$

From Figure 9, $d_t = E_t v_t$, therefore:

$$v_t = (1 + S_t E_t + G_t H_t E_t)^{-1} G_t v_0 \quad (19)$$

The goal is to choose a class of compensators, H_t , to shape the impedance of the system, $E_t [1 + S_t E_t + G_t H_t E_t]^{-1} G_t$, in equation 18. The small value for H_t in a particular direction implies a very stiff velocity control system. In the limit, when H_t is chosen to be zero in a particular direction, the system behaves as a velocity control in that direction. When H_t is chosen to be a large number, the system will be very compliant in tangential direction and small contact forces will be generated. In the deburring process we plan to modulate H_t such that it has a large value in the direction tangential to the part while the system is stable.

To guarantee the stability of the closed-loop system in the nonlinear case, H_t must be chosen such that (11):

$$\|H_t\|_P \|\omega_t(e_t)\|_P < 1 \quad (20)$$

Inequality 20 states that the L_P -norm of H_t must be less than the reciprocal of the "magnitude" of the mapping in the forward loop in Figure 9 where $\|\cdot\|_P$ represents the P -norm of a function. $\omega_t(e_t)$ is the mapping from e_t to v_t . In the linear case, $\omega_t = E_t (S_t E_t + 1)^{-1} G_t$ where all the operators in the system are linear transfer functions. The stability criteria for linear system is:

$$|H_t| < |G_t^{-1} (S_t + 1/E_t)| \quad (21)$$

where $|\cdot|$ denotes the magnitude of the transfer function. The smaller the sensitivity of the robot manipulator is, the smaller H_t must be chosen. Also from inequality 21, the more rigid the part is, the smaller H_t must be chosen.

4. Emerging the Deburring and Tracking

The XY table in Figure 10 is used to employ the above tracking and deburring methods in deburring the parts with unknown geometry. The workpiece to be deburred is mounted on the XY table for maneuvering while the grinder is held vertically by a stationary platform. The sample part is mounted on the table by a sample holder. Depending on the geometry of the sample part, various sample holders can be made. We admit that in the actual deburring process, it may be better to move the grinder with the robot while the part is on a stationary platform. Reference 9 describes an active end-effector that can be held by commercial robot manipulators. As you see in Figure 10, two force sensors are used in this operation. One force sensor is installed on the tool holder for measurement of tracking force, t , while another force sensor is installed under the part for measurement of the deburring force, d . Note that the use of two sensors in this architecture is necessary. We cannot use the normal deburring force in tracking algorithm. If the normal deburring force is used in tracking algorithm, the tool will follow the contour of the burr and rounded burr will be developed.

The XY table is interfaced to a micro computer for

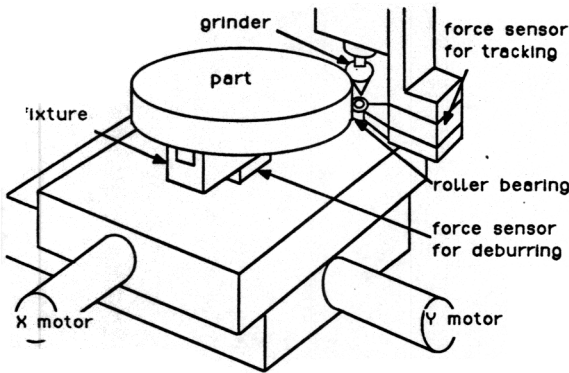


Figure 10: The XY Table Used as a Two Dimensional Robot to Maneuver the Part

control. The control algorithms of the tracking and deburring were implemented on the XY table via the μ -computer. H_t and H_n are chosen to satisfy inequalities 21. Because of the lead screw mechanism in the XY table drive, S_t and S_n , the sensitivity of the XY table is very small. H_t must be chosen such that $|G_t H_t| < |1/E_t|$. Since $1/E_t$ is measured as $1/69.8$ nt/cm/sec, therefore H_t is chosen such that the entire loop transfer function $G_t H_t$ has the magnitude of less than $1/69.8$ nt/cm/sec. The structure of H_t is not of importance as long as its magnitude is such that $|G_t H_t| < |1/E_t|$. Figure 11 shows the frequency response of table, (G_t), in the tangential direction. As seen in Figure 11, the input velocity command is equal to the output velocity command for about 35 hertz. H_t can be chosen as any transfer function as long as $|G_t H_t| < |1/E_t|$.

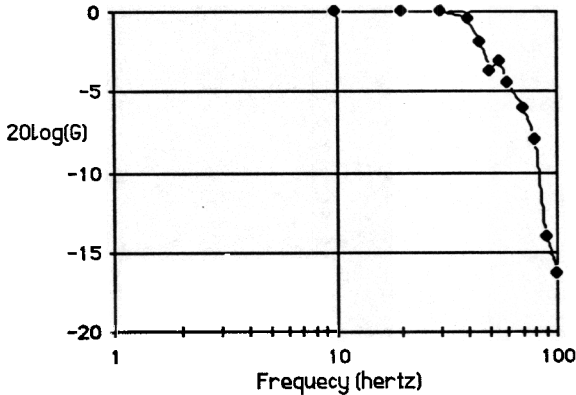


Figure 11: Frequency Response of G_t

The objective of this experiment is to substantiate the size of the cutting forces in a edge deburring when the above method control is employed to control the XY table. The edge of the sample part has been filed to produce step burrs as shown in Figure 12.

Figure 13 shows the tangential and normal force when no force control is employed in the tangential direction. The grinder is driven with constant velocity along the edge of the part. As seen in Figure 13, once the grinder encounters the burr, the tangential force increased to 25 nt and the deburring tool stalled. Figure 14 shows the tangential and normal forces when a force control strategy according to Figure 9 is employed in deburring the same size burr (depth of cut = .045"). H_t in the direction normal to the part is chosen to be zero. H_t in the direction tangential to the part is chosen to be a large number while satisfying inequality 5. The commanded tangential force is 5 nt and the average speed is 0.088 in/sec. Figure 12 shows the tangential and

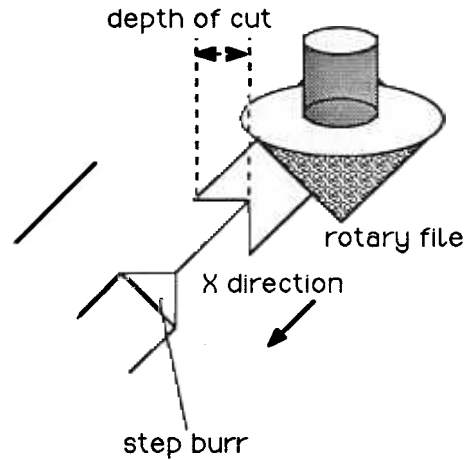


Figure 12: The Sample Part With Step Burr

normal force with the same commanded force in the tangential direction when a burr with the depth of cut of .06" is used. Since the tangential force remains constant at 5 nt, the average speed of the system decreases from .088 in/sec to .057 in/sec. Since the tangential force is kept constant by the force control system, therefore the MRR is constant also. The ratio of the velocities (.088/.057=1.6) is inversely equal to the tangential area ratio (.06/.045)²=1.7

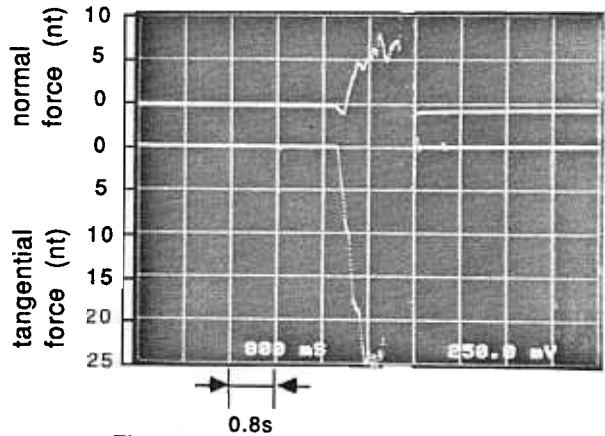


Figure 13: No force control, tool stalled depth of cut: .045"

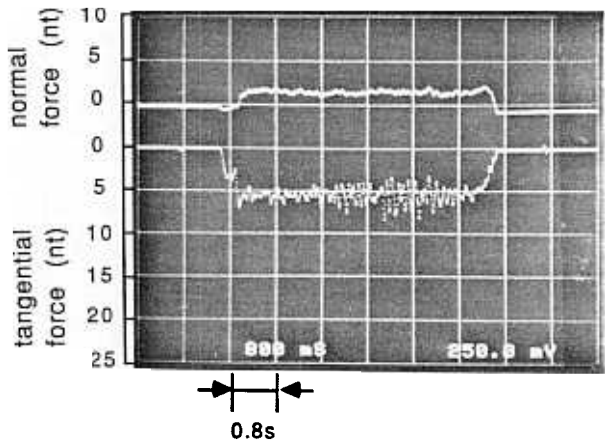


Figure 14 : Force control in effect depth of cut: .045", average speed: .088 in/sec

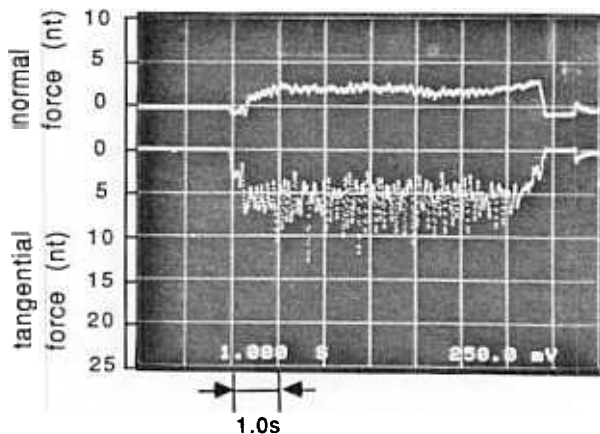


Figure 15: Force control in effect, depth of cut: .06"
average speed: .057 in/sec

5. Summary and Conclusion

Two problems have been addressed in this paper: tracking the part contour, and control of the metal removal process. The tracking control employs the force measured by a force sensor to find the normal to the part surface, while the deburring algorithm uses another set of contact forces (cutting forces generated by the cutter) to develop a stable metal removal. The use of two sensors in this architecture is necessary. One cannot use the normal deburring force in tracking algorithm. If the normal deburring force is used in tracking algorithm, the tool will follow the contour of the burr and rounded burr will be developed.

References

- 1) Asada, H., Kazuo, O., "On the Dynamic Analysis of a Manipulator and its End Effector", IEEE Conference on Robotics and Automation, April 1987, Raleigh, North Carolina.
- 2) Bausch, J. J., Kramer, B. M., Kazerooni, H., "Compliant Tool Holders for Robotic Deburring", ASME Winter Annual Meeting, December 1986.
- 3) Dornfeld, D. A., Masaki, T., "Acoustic Emission Feedback for Deburring Automation", ASME Winter Annual Meeting, Dec. 1987.
- 4) Hollowell, R., "An Analysis of Robotic Chamfering and Deburring", ASME Winter Annual Meeting, Dec. 1987.
- 5) Kazerooni, H., Sheridan, T. B., Houpt, P.K. "Fundamentals of Robust Compliant Motion for Robot Manipulators", IEEE Journal on Robotics and Automation, Volume 2, Number 2, June 1986.
- 6) Kazerooni, H., Houpt, P. K., Sheridan, T. B., "A Design Method for Robust Compliant Motion for Manipulators", IEEE Journal on Robotics and Automation, Volume 2, Number 2, June 1986.
- 7) Kazerooni, H., Bausch, J. J., Kramer, B. M., "Automated Deburring by Robot Manipulators", Journal of Dynamic Systems Measurements and Control, December 1986.
- 8) Kazerooni, H., "Robust nonlinear Impedance Control for Robot Manipulators", IEEE Conference on Robotics and Automation, April 1987, Raleigh, North Carolina.
- 9) Kazerooni, H., Guo, J., "Design and Control of the Active Compliant End-Effector", American Control Conference, June 1987, Minneapolis, Minnesota, June 1987.
- 10) Kazerooni, H., "Hybrid Force/Position Control in Robotic Deburring", ASME Winter Annual Meeting, Dec. 1987.
- 11) Kazerooni, H., Tsay, T. I., "Stability Criteria for Robot Compliant Maneuvers", IEEE Conference on Robotics and Automation, April 88, Philadelphia, PA.
- 12) Paul, F. W., FitzPatrick, P. R., "Dynamic System Analysis of Robot Assisted Brush Finishing", ASME Winter Annual Meeting, Dec. 1987.
- 13) Vidyasagar, M., Spong, M. W., "Robust Nonlinear Control of Robot Manipulators", CDC, December 1985.
- 14) Whitney, D. E., "Force-Feedback Control of Manipulator Fine Motions", ASME Journal of Dynamic Systems, Measurements and Control, June 1977.